



# Continuous-wave and passively Q-switched cryogenic Yb:KLu(WO<sub>4</sub>)<sub>2</sub> laser

PETR NAVRATIL,<sup>1</sup> VENKATESAN JAMBUNATHAN,<sup>1,\*</sup> SAMUEL PAUL DAVID,<sup>1</sup> FANGXIN YUE,<sup>1,2</sup> JOSEP MARIA SERRES,<sup>3</sup> XAVIER MATEOS,<sup>3,4</sup> MAGDALENA AGUILÓ,<sup>3</sup> FRANCESC DÍAZ,<sup>3</sup> UWE GRIEBNER,<sup>4</sup> VALENTIN PETROV,<sup>4</sup> ANTONIO LUCIANETTI,<sup>1</sup> AND TOMAS MOCEK<sup>1</sup>

<sup>1</sup>HiLASE Centre, Institute of Physics CAS, Za Radnicí 828, 25241 Dolní Břežany, Czech Republic

<sup>2</sup>Czech Technical University in Prague, Břehová 7, 11519 Prague 1, Czech Republic

<sup>3</sup>Física i Cristal·lografia de Materials i Nanomaterials (FiCMA-FiCNA)-EMaS, Universitat Rovira i Virgili, Campus Sescelades, c/Marcel·lí Domingo, s/n., E-43007 Tarragona, Spain

<sup>4</sup>Max Born Institute for Nonlinear Optics and Short Pulse Spectroscopy, Max-Born-Str. 2a, D-12489 Berlin, Germany

\*jambunath@fzu.cz

**Abstract:** We study cryogenic laser operation of an Yb-doped KLu(WO<sub>4</sub>)<sub>2</sub> crystal pumped with a volume Bragg grating (VBG) stabilized diode laser at 981 nm. In the continuous wave laser regime, a maximum output power of 4.31 W is achieved at 80 K with a slope efficiency of 44.0% with respect to the incident pump power. Using a 85% initial transmission Cr:YAG crystal for passive Q-switching, an average output power of 2.11 W is achieved at 100 K for a repetition rate of 19 kHz. The pulse energy, pulse duration and peak power amount to 111 μJ, 231 ns and 0.48 kW, respectively.

© 2017 Optical Society of America

**OCIS codes:** (140.3380) Laser materials; (140.3615) Lasers, ytterbium; (140.3480) Lasers, diode-pumped.

## References and links

1. S. Chenais, F. Druon, S. Forget, F. Balembois, and P. Georges, "On thermal effects in solid-state lasers: The case of ytterbium-doped materials," *Prog. Quantum Electron.* **30**(4), 89–153 (2006).
2. T. Y. Fan, D. J. Ripin, R. L. Aggarwal, J. R. Ochoa, B. Chann, M. Tillemann, and J. Spitzberg, "Cryogenic Yb<sup>3+</sup>-doped solid-state lasers," *IEEE J. Sel. Top. Quantum Electron.* **13**(3), 448–459 (2007).
3. D. C. Brown, "The promise of cryogenic solid-state lasers," *IEEE J. Sel. Top. Quantum Electron.* **11**(3), 587–599 (2005).
4. R. L. Aggarwal, D. J. Ripin, J. R. Ochoa, and T. Y. Fan, "Measurement of thermo-optic properties of Y<sub>3</sub>Al<sub>5</sub>O<sub>12</sub>, Lu<sub>3</sub>Al<sub>5</sub>O<sub>12</sub>, YAlO<sub>3</sub>, LiYF<sub>4</sub>, LiLuF<sub>4</sub>, BaY<sub>2</sub>F<sub>8</sub>, KGd(WO<sub>4</sub>)<sub>2</sub>, and KY(WO<sub>4</sub>)<sub>2</sub> laser crystals in the 80–300 K temperature range," *J. Appl. Phys.* **98**(10), 103514 (2005).
5. D. C. Brown, R. L. Cone, Y. C. Sun, and R. W. Equall, "Yb:YAG absorption at ambient and cryogenic temperatures," *IEEE J. Sel. Top. Quantum Electron.* **11**(3), 604–612 (2005).
6. J. Korner, V. Jambunathan, J. Hein, R. Seifert, M. Loeser, M. Siebold, U. Schramm, P. Sikocinski, A. Lucianetti, T. Mocek, and M. C. Kaluza, "Spectroscopic characterization of Yb<sup>3+</sup>-doped laser materials at cryogenic temperatures," *Appl. Phys. B* **116**(1), 75–81 (2014).
7. L. E. Zapata, D. J. Ripin, and T. Y. Fan, "Power scaling of cryogenic Yb:LiYF<sub>4</sub> lasers," *Opt. Lett.* **35**(11), 1854–1856 (2010).
8. S. Ricaud, D. N. Papadopoulos, P. Camy, J. L. Doualan, R. Moncorgé, A. Courjaud, E. Mottay, P. Georges, and F. Druon, "Highly efficient, high-power, broadly tunable, cryogenically cooled and diode-pumped Yb:CaF<sub>2</sub>," *Opt. Lett.* **35**(22), 3757–3759 (2010).
9. L. D. Merkle, G. A. Newburgh, N. Ter-Gabrielyan, A. Michael, and M. Dubinskii, "Temperature-dependent lasing and spectroscopy of Yb:Y<sub>2</sub>O<sub>3</sub> and Yb:Sc<sub>2</sub>O<sub>3</sub>," *Opt. Commun.* **281**(23), 5855–5861 (2008).
10. V. Jambunathan, L. Horackova, P. Navratil, A. Lucianetti, and T. Mocek, "Cryogenic Yb:YAG laser pumped by VBG-stabilized narrowband laser diode at 969 nm," *IEEE Photonics Technol. Lett.* **28**(12), 1328–1331 (2016).
11. V. Petrov, M. C. Pujol, X. Mateos, Ö. Silvestre, S. Rivier, M. Aguiló, R. M. Solé, J. Liu, U. Griebner, and F. Díaz, "Growth and properties of KLu(WO<sub>4</sub>)<sub>2</sub>, and novel ytterbium and thulium lasers based on this monoclinic crystalline host," *Laser Photonics Rev.* **1**(2), 179–212 (2007).
12. V. Jambunathan, X. Mateos, M. C. Pujol, J. J. Carvajal, C. Zaldo, U. Griebner, V. Petrov, M. Aguiló, and F. Díaz, "Crystal growth, optical spectroscopy, and continuous-wave laser operation of Ho:KLu(WO<sub>4</sub>)<sub>2</sub> crystals," *Appl. Phys. B* **116**(2), 455–466 (2014).

13. Z. H. Cong, Z. J. Liu, Z. G. Qin, X. Y. Zhang, H. J. Zhang, J. Li, H. H. Yu, and W. T. Wang, "LD-pumped actively Q-switched Nd:KLu(WO<sub>4</sub>)<sub>2</sub> self-Raman laser at 1185 nm," *Opt. Laser Technol.* **73**, 50–53 (2015).
14. J. M. Serres, P. Loiko, X. Mateos, K. Yumashev, N. Kuleshov, V. Petrov, U. Griebner, M. Aguiló, and F. Díaz, "Prospects of monoclinic Yb:KLu(WO<sub>4</sub>)<sub>2</sub> crystal for multi-watt microchip lasers," *Opt. Mater. Express* **5**(3), 661–667 (2015).
15. O. Silvestre, J. Grau, M. C. Pujol, J. Massons, M. Aguiló, F. Díaz, M. T. Borowiec, A. Szewczyk, M. U. Gutowska, M. Massot, A. Salazar, and V. Petrov, "Thermal properties of monoclinic KLu(WO<sub>4</sub>)<sub>2</sub> as a promising solid state laser host," *Opt. Express* **16**(7), 5022–5034 (2008).
16. M. Segura, M. Kadankov, X. Mateos, M. C. Pujol, J. J. Carvajal, M. Aguiló, F. Díaz, U. Griebner, and V. Petrov, "Polarization switching in the 2- $\mu$ m Tm:KLu(WO<sub>4</sub>)<sub>2</sub> laser," *Laser Phys. Lett.* **9**(2), 104–109 (2012).
17. P. A. Loiko, X. Mateos, N. Kuleshov, A. A. Pavlyuk, K. V. Yumashev, V. Petrov, U. Griebner, M. Aguiló, and F. Díaz, "Thermal-lens-driven effects in N<sub>g</sub>-cut Yb –and Tm-doped monoclinic KLu(WO<sub>4</sub>)<sub>2</sub>," *IEEE J. Quantum Electron.* **50**, 669–676 (2014).
18. P. Navratil, V. Jambunathan, L. Horackova, A. Lucianetti, and T. Mocek, "Diode pumped compact cryogenic Yb:YAG/Cr:YAG pulsed laser," *Proc. SPIE* **9726**, 97261G (2016).

## 1. Introduction

In a quasi-three level solid-state laser system at room temperature (RT), the Stark levels of the ground state are partially populated including the lower laser level. An important example of such a quasi-three level laser system is the one based on the trivalent ytterbium (Yb<sup>3+</sup>) ion. The simple energy level structure of Yb<sup>3+</sup> consisting of only two electronic states prevents excited state absorption (ESA) or up-conversion (UC) losses. The very small Stokes shift (quantum defect) is a consequence of this simple structure and offers attractive power scaling capabilities. Nevertheless, the above-mentioned thermal population of the lower laser level is inevitable in the case of small quantum defects and leads to reabsorption losses limiting the overall efficiency of the laser and mitigating the power scaling capabilities [1].

Many laser materials suffer from low transition cross-sections, such as the widely known Yb:YAG laser. The strategy to cool the active medium down to cryogenic temperatures partially overcomes the above issues related to reabsorption and low cross-sections. The cross sections increase at low temperatures. In addition, at cryogenic temperatures the thermo-optical properties are enhanced. The thermal conductivity increases while the thermal expansion as well as the thermal dependence of the refractive index ( $dn/dt$ ) decrease notably. All these factors affect directly the reduction of the thermal lens effect occurring in the active medium. The improvement of the thermo-optical properties results in higher laser efficiencies, in particular the optical-to-optical efficiency in relation to the reduced laser threshold, and also facilitates scaling of the average output power [2–6].

To date, many Yb<sup>3+</sup> doped laser hosts have been studied at cryogenic temperatures [7–10] while little attention has been paid to the Yb-doped KLu(WO<sub>4</sub>)<sub>2</sub> crystal (hereafter KLuW). KLuW belongs to the family of monoclinic potassium double tungstates, having chemical formula KRE(WO<sub>4</sub>)<sub>2</sub>, (RE = Y, Gd, Lu). It exhibits favorable polarized spectroscopic properties when doped with rare earth ions (e.g. Yb<sup>3+</sup>, Tm<sup>3+</sup>, Ho<sup>3+</sup>) [11,12] due to the strong anisotropy. It is characterized by higher absorption and stimulated-emission cross-sections (compared to YAG) and can accommodate highest density of dopant ions without concentration quenching giving the possibility to reduce the thickness of the active medium while keeping a reasonable absorption. Furthermore, KLuW exhibits a strong stimulated Raman scattering effect. It acts as self-Raman laser material with potential of generating additional wavelengths beside the fundamental laser wavelength [13]. Moderate output power levels have been demonstrated with Yb<sup>3+</sup>, Tm<sup>3+</sup> or Ho<sup>3+</sup> dopings at RT using different cavity configurations [11,14]. However, KLuW suffers from relatively poor thermo-optical properties at RT, especially moderate thermal conductivity and high thermal expansion coefficient [15]. The thermal conductivity of undoped KLuW ( $\sim 3$  W/m/K) is about four times lower than that of YAG ( $\sim 14$  W/m/K). As a consequence, the laser beam quality is affected during power scaling due to thermal distortions in the gain medium and polarization switching can occur due to the enhancement of the thermal lens [14,16]. The situation can be greatly improved employing the athermal cut concept, where the impact of the negative  $dn/dt$

of KLuW compensates the positive thermal expansion providing a near-zero and a slightly positive temperature-induced change of the optical path. For this purpose the propagation direction has to be along the  $N_g$  principal optical direction in the dielectric frame of KLuW and  $\text{KRE}(\text{WO}_4)_2$  in general [17].

In order to reduce the negative impact of the thermal effects at RT and take advantage of the above mentioned spectroscopic and thermo-optical properties, in this work we study the performance of the Yb:KLuW laser at cryogenic temperatures. The laser is pumped by a Volume Bragg Grating (VBG) stabilized laser diode emitting at 981 nm. In addition, passive Q-switching of the laser using different initial transmission of the Cr:YAG crystals employed as saturable absorbers (SA) is also studied.

## 2. Experimental setup

The laser setup for the cryogenic laser experiments is formed by an L-shaped cavity as shown in Fig. 1. It consists of a high reflection (HR) coated for 1030 nm concave mirror (M1) having radius of curvature  $-300$  mm, a plane dichroic bending mirror (M2), HR (s-polarization) coated for the 1020 – 1200 nm range on the front side and anti-reflection (AR) coated for the 900 – 980 nm range on the rear side, a plano convex lens AR coated for 1030 nm (L3) having focal length of 150 mm and a series of plane output couplers (M3) with transmission  $T_{\text{OC}} = 2, 5, 10, 20, 30$  and 50% in the 1020 – 1070 nm spectral range. The fiber-coupled laser diode stabilized at 981 nm by a VBG, (BWT Beijing LTD), delivered a maximum output power of 27 W with a 0.2 nm spectral bandwidth. The fiber core had a diameter of 105  $\mu\text{m}$  with a numerical aperture,  $\text{NA} = 0.22$ . The unpolarized output from the fiber was imaged using AR coated achromatic lenses L1 and L2, with a 1:2 magnification ratio resulting in a pump beam diameter of 210  $\mu\text{m}$  in the crystal.

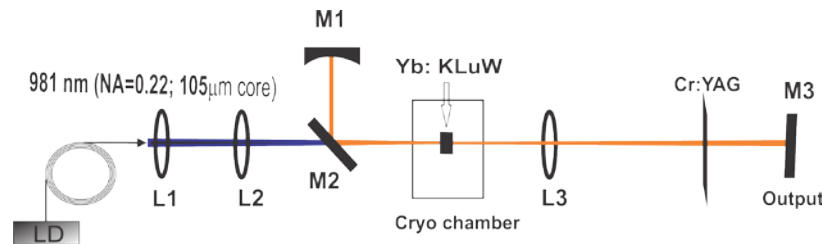


Fig. 1. Laser setup: L1, L2 achromatic lenses (150 and 300 mm focal lengths), M1 – concave mirror (radius of curvature =  $-300$  mm), M2 – dichroic mirror, L3 – plano convex lens (150 mm focal length), M3 – plane output coupler.

An uncoated  $N_g$ -cut 5 at.% Yb:KLuW crystal, with a thickness of 1.85 mm and an aperture of  $5 \times 5$   $\text{mm}^2$  was employed as an active medium. Passive Q-switching was realized using AR coated Cr:YAG SAs exhibiting three different initial transmissions,  $T_0 = 85\%$ , 90% and 95%. The thickness of the 5-mm diameter plates was 1.60, 1.55 and 1.45 mm, respectively.

The Yb:KLuW crystal was mounted in a brass holder at normal incidence with the unpolarized pump light propagating along the  $N_g$  principal optical direction. Efficient cooling of the sample was provided by placing the brass holder in a cryogenic vacuum chamber connected to a cryostat (Cryodyne, model no: 22C) that contains a two-stage closed cycle helium gas circuit. The heat load of the cryostat was 8 W at 100 K. To stabilize and monitor the temperature precisely, a temperature controller (Lakeshore, model no: 335) was used. It included a 50-Ohm resistor for heating and two silicon diode sensors (model no: DT 670) connected to the sample and the cold finger.

To characterize the passively Q-switched pulses, a fast photodiode (Alphas, model: UPD-500-UP) and an oscilloscope (Tektronix, model: DPO 5204 B) were used providing a temporal resolution of 500 ps. The emission from the diode laser and the optical density

(absorption) of Yb:KLuW at different temperatures illuminating the sample by a white light source were measured by a high resolution spectrophotometer (Horiba Jobin Yvon, model no: 1250M) which included a diffraction grating of 600 grooves/mm blazed at 1  $\mu\text{m}$  and a photomultiplier tube (Hamamatsu, model no: H10330A-25), sensitive in the 950 – 1200 nm spectral range.

The cavity was optimized for maximum output power by adjusting the separations between the optical elements. The measured optimum total cavity length was 754.8 mm, which includes 300 mm from M1 to the pump side of the sample, 153 mm from the other side of the sample to L3, and 300 mm from L3 to M3. The SA was placed at 200 mm from L3 for the Q-switching experiments. Using ABCD-matrix formalism, the estimated mode size was  $\sim 220 \mu\text{m}$  in the crystal.

### 3. Results and discussion

#### 3.1 Cryogenic continuous-wave Yb:KLuW laser

The input-output characteristics of the continuous-wave (CW) cryogenic Yb:KLuW laser were studied in two ways. At first the laser performance (output power, laser threshold and slope efficiency) was characterized at fixed temperature for different transmission of the output coupler. In the second series of measurements, the temperature was varied at a fixed output coupler transmission ( $T_{\text{OC}} = 20\%$ ).

In the first experiments, we fixed the temperature of the sample to 100 K and varied the transmittance of output coupler  $T_{\text{OC}} = 2\%$ , 5%, 10%, 20%, 30% and 50%. Figure 2(a) shows the CW input-output characteristics of the Yb:KLuW laser. The output power linearly increases without any thermal effect up to the highest available pump power. The laser threshold increases with the increase in transmission of the output coupler, which is usual when the cavity losses increase. The highest slope efficiency and output power are 39.7% and 3.87 W, respectively, achieved at an incident power of 10.93 W for  $T_{\text{OC}} = 20\%$ . The rest of the output couplers showed inferior slope efficiency and output power. In our experiments, the pump power was limited to 10.93 W, where the sample temperature starts fluctuating by  $\sim 20$  K due to the limited heat load of the cryostat used.

To study the effect of temperature on the laser performance, we chose the output coupler with the best results,  $T_{\text{OC}} = 20\%$ . The temperature was varied from 80 to 300 K with steps of 20 K. Figure 2(b) shows the input-output characteristics of the Yb:KLuW laser at various temperatures. For clarity, only the data series in steps of 40 K are plotted. The output power linearly increases with the incident pump power and the slope efficiency increases with the decrease of the sample temperature. A maximum output power of 4.31 W with a slope efficiency of 44.0% was achieved for 80 K. The output was always linearly polarized with  $E//N_m$ , in agreement with the polarization dependence of the gain cross section [11].

We attribute the better laser performance at cryogenic temperature with respect to RT to a significant reduction of the reabsorption at the laser wavelength. However, a further decrease of the reabsorption shall be possible since the concentration of Yb in the crystal is rather high, i.e. 5 at.%. Samples with lower doping could greatly improve the laser performance.

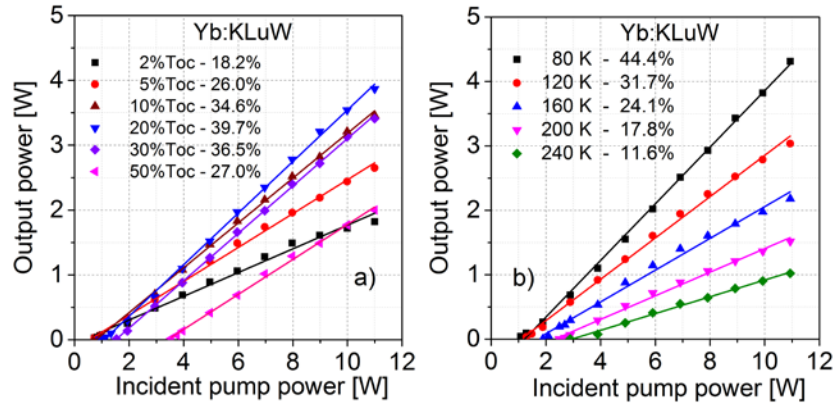


Fig. 2. Input-output power characteristics of the CW cryo-cooled Yb:KLuW laser (a) at 100 K for different output coupler transmission and (b) for  $T_{OC} = 20\%$  varying the sample temperature.

The thermal dependence of laser threshold and the slope efficiency of the cryogenic Yb:KLuW laser for  $T_{OC} = 20\%$  is shown in Fig. 3(a). From Fig. 3(a), it becomes evident that the laser threshold decreases and the slope efficiency increases more than four times when the sample is cooled down from RT to 80 K. Figure 3(b) shows the temperature dependence of the laser wavelength. The laser wavelength shifted from 1030 to 1024 nm when the Yb:KLuW crystal was cooled down from 260 K to 80 K. This is a clear evidence of a reduction of the reabsorption losses. We measured an excellent Gaussian beam profile at 100 K, depicted as an inset in Fig. 3(b). Thus, it can be concluded that the significant temperature dependence of the CW laser performance is due both to a transition to a four-level system at low temperatures and to an improvement of the thermo-mechanical and thermo-optic properties of KLuW although it is impossible to separate and quantify the contributions of these effects from such experiments.

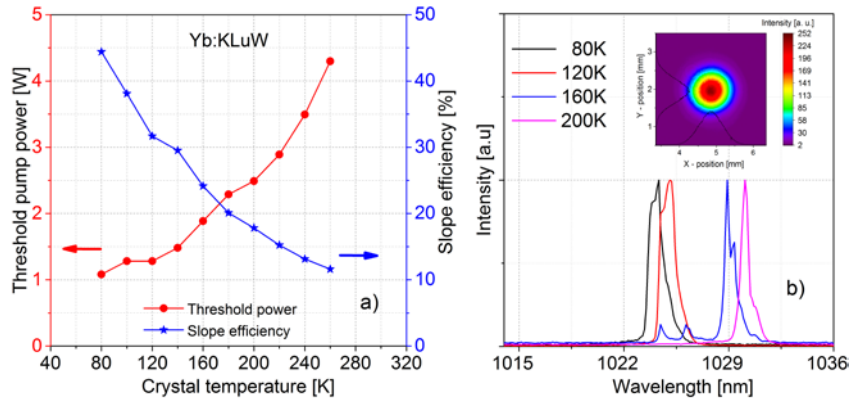


Fig. 3. (a) Dependence of laser threshold and slope efficiency versus temperature of the cryogenic Yb:KLuW laser ( $T_{OC} = 20\%$ ) and (b) Laser emission wavelength at various temperatures ( $T_{OC} = 20\%$ ); inset: beam profile recorded at 100 K.

### 3.2 Effect of the crystal absorption on the Yb:KLuW laser performance

To assess the effect of the pump absorption in the crystal, it was measured in non-lasing conditions versus incident pump power for different crystal temperatures as shown in Fig. 4(a).

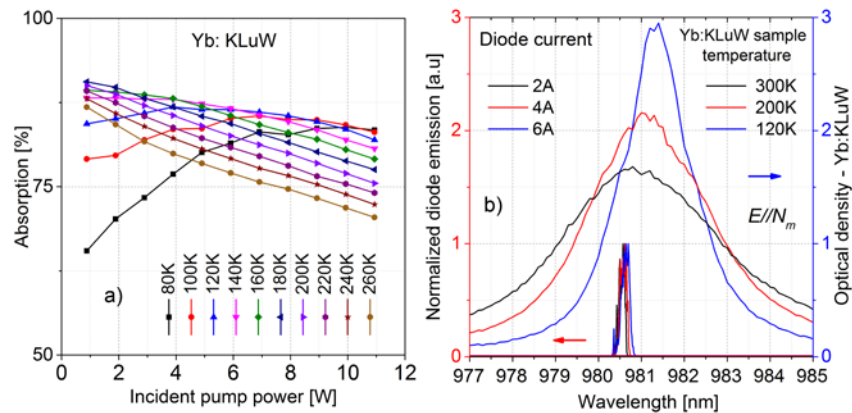


Fig. 4. (a) Yb:KLuW pump absorption versus incident power for different crystal temperatures and (b) VBG stabilized 981 nm diode laser emission for various current levels, *left* and Yb:KLuW optical density at different crystal temperatures, *right*.

From Fig. 4(a) it can be seen that the pump absorption in the crystal is lower at low incident pump power for temperatures below 120 K. To verify the reason for this lower absorption, we measured the emission wavelength of the pump diode at different current levels and for different crystal temperatures as shown in Fig. 4(b). The peak wavelength of the diode shifted from 980.55 to 980.65 nm with the increase of the diode current whereas the peak absorption wavelength of the Yb:KLuW crystal was centered at 981.2 nm with a full width at half maximum (FWHM) of 1.5 nm at 120 K. As can be seen from Fig. 4(b), the absorption peak is red shifted with the decrease in temperature. This leads to a mismatch between the diode laser pump emission and the absorption band of Yb:KLuW (the dominant part of which is for polarization  $E//N_m$ ). For temperatures below 120 K, the diode emission is at the edge of the absorption band of Yb:KLuW which leads to a drop in absorption for lower temperatures. This observation emphasizes the crucial importance of pump source linewidth and peak wavelength at cryogenic temperatures.

### 3.3 Passive Q-switching of the cryogenic Yb:KLuW laser with Cr:YAG as a saturable absorber

Passive Q-switching of the cryogenic Yb:KLuW laser was realized using AR coated Cr:YAG as a SA with different initial transmissions  $T_0 = 85\%$ ,  $90\%$  and  $95\%$ . The temperature of the sample and transmission of output coupling was fixed at 100 K and 20% respectively for the first experiments.

The average output power, the pulse width and the repetition rate of the passively Q-switched Yb:KLuW laser at 100 K are shown in Fig. 5(a) versus incident pump power. As anticipated, the average output power increases with the SA transmission. The maximum achieved average output power amounts to  $\sim 2.8$  W for  $T_0 = 95\%$ . In Fig. 5(b), the pulse width remains almost constant for incident powers greater than 6 W with a minimum pulse width of 231 ns for the  $T_0 = 85\%$  SA. The shortest pulse duration corresponds to the absorber with the highest modulation depth. The repetition rate increases with the incident power. It is higher for higher transmission of the SA, which can be attributed to its faster bleaching.

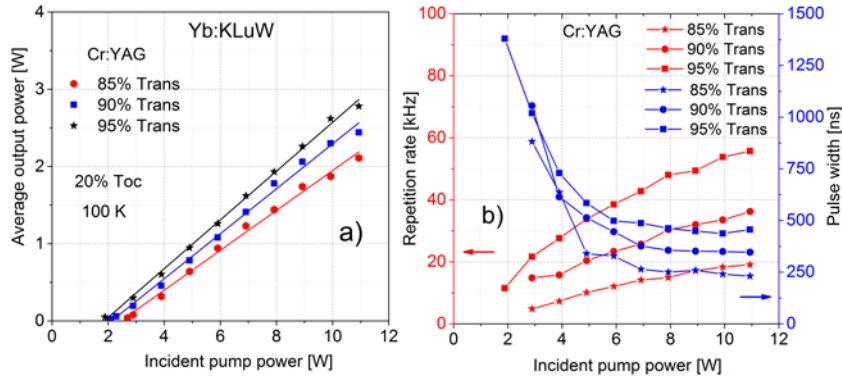


Fig. 5. Cryogenic Yb:KLuW laser, passively Q-switched by Cr:YAG saturable absorbers with different initial transmissions: (a) Average output power versus incident pump power; (b) Repetition rate and pulse width (FWHM) versus incident pump power.

The calculated pulse energy and peak power resulting from Figs. 5(a) and 5(b) are depicted in Fig. 6(a) for different  $T_0$ , indicating a maximum pulse energy exceeding 0.1 mJ. The pulse train and a single pulse trace for the  $T_0 = 85\%$  SA at an incident pump power of 10.9 W are shown in Fig. 6(b). For the passively Q-switched regime, the laser emission wavelength was always 1025 nm and the laser polarization remained  $E//N_m$ . Details of the pulsed laser characteristics are summarized in Table 1. Further shortening of the pulses is anticipated by lowering the initial transmission of the Cr:YAG (75 or 70%) or by shortening the cavity length using a modular setup [18]. This will simultaneously reduce the repetition rate and increase the single pulse energy and the peak power.

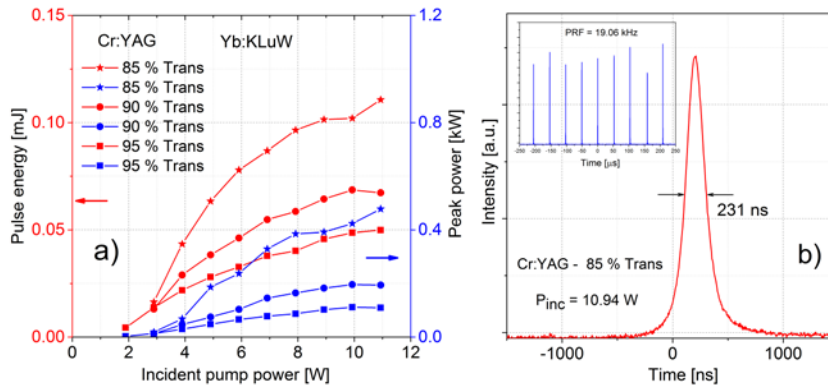


Fig. 6. (a) Calculated pulse energy and peak power versus incident pump power of the the cryogenic Yb:KLuW laser with different  $T_0$  of the Cr:YAG. (b) Single pulse with temporal width of 231 ns and an oscilloscope trace of the pulse train at an incident pump power of 10.94 W using the  $T_0 = 85\%$  SA.

Table 1. Output characteristics of the passively Q-switched cryogenic Yb:KLuW laser with different initial transmission of the Cr:YAG saturable absorber

Initial transmission SA [%]	Average output power [W]	Slope efficiency [%]	Pulse width [ns]	Repetition rate [kHz]	Energy [ $\mu$ J]	Peak power [kW]
85	2.11	26.0	231	19.0	111	0.48
90	2.44	29.0	347	36.2	67	0.19
95	2.78	31.5	456	55.7	50	0.11

#### 4. Conclusion

In conclusion, as a proof of principle we demonstrated substantial improvement of the laser operation characteristics of Yb-doped  $\text{KLu}(\text{WO}_4)_2$  at cryogenic temperatures using a VBG stabilized laser diode emitting at 981 nm as a pump source. In the CW laser regime a maximum output power of 4.31 W with a slope efficiency of 44.0% was achieved at 80 K. In passively Q-switched operation at 100 K, an average output power of 2.11 W at a repetition rate of 19 kHz was achieved using a 85% initial transmission Cr:YAG saturable absorber. The maximum pulse energy, shortest pulse width and maximum peak power obtained were 111  $\mu\text{J}$ , 231 ns and 0.48 kW respectively. Future work will focus on the optimization of the active medium to operate at cryogenic temperatures in terms of doping level and thickness, as well as, on the optimization of the SA characteristics. We anticipate, AR coated Yb:KLuW samples and a higher heat load cryostat will enable substantial power and energy scaling beyond the state-of-the-art of existing Yb:KREW lasers demonstrated so far at RT, maintaining the excellent beam quality.

#### Funding

This work was co-financed by the European Regional Development Fund and the state budget of the Czech Republic (project HiLASE CoE: Grant No. CZ.02.1.01/0.0/0.0/15\_006/0000674), by the European Union's Horizon 2020 research and innovation programme under grant agreement No. 739573, by the Ministry of Education, Youth and Sports of the Czech Republic (Programmes NPU I Project No. LO1602, and Large Research Infrastructure Project No. LM2015086). This work was also supported in part by the Spanish Government under projects MAT2016-75716-C2-1-R (AEI/FEDER,UE), MAT2013-47395-C4-4-R, TEC 2014-55948-R and by the Generalitat de Catalunya under project 2014SGR1358.

#### Acknowledgments

F. D. acknowledges additional support through the ICREA academia award 2010ICREA-02 for excellence in research. X. M. acknowledges support from the European Union's Horizon 2020 research and innovation programme under the Marie Skłodowska-Curie grant agreement No 657630.